THESIS

INTEGRATION OF VARIABLE PHOTOSYNTHETIC CAPACITY

INTO A BIOGEOCHEMICAL MODEL

Submitted by

Jonathan R. Straube

Graduate Degree Program in Ecology

In partial fulfillment of the requirements

For the Degree of: Master of Science

Colorado State University

Fort Collins, Colorado

Fall 2011

Master's Committee:

    Advisor: Dennis S. Ojima

    William J. Parton
    Patrick J. Burns

ABSTRACT

INTEGRATION OF VARIABLE PHOTOSYNTHETIC CAPACITY

INTO A BIOGEOCHEMICAL MODEL

We integrated a photosynthetic sub-model into the daily Century model, DayCent, to improve the estimations of carbon fluxes at the Niwot Ridge LTER site; the new version is called DayCent-Photosyn. The photosynthetic sub-model, adapted from the SIPNET/PnET family of models, includes solar radiation and vapor pressure deficit controls on production, as well as temperature and water stress terms. A key feature we added to the base photosynthetic equations is the addition of a variable maximum net photosynthetic rate (*Amax*). We optimized the parameters controlling photosynthesis using a variation of the Metropolis-Hastings algorithm along with data-assimilation techniques. The model was optimized and validated against level 4 data available from the Ameriflux website using observed net ecosystem exchange (NEE) and estimated gross primary production (GPP) and ecosystem respiration (R_e) values. The inclusion of a variable *Amax* rate greatly improved model performance (NEE RMSE = 0.63 gC m^{-2}, AIC= 2099) versus a version with a single *Amax* parameter (NEE RMSE = 0.74 gC m^{-2}, AIC= 3724). DayCent-Photosyn is able to capture the inter-annual and seasonal flux patterns, including the critical early season assimilation, but tends to overestimate yearly

NEE uptake. The simulated influence of a variable *Amax* rate suggest a need for further studies on the process controls affecting the seasonal photosynthetic rates.

TABLE OF CONTENTS

INTRODUCTION

Background Information

Terrestrial ecosystems serve as a biological pump for CO_2, exchanging over 90 Gt of C per year in CO_2 through photosynthesis and respiration processes (Schimel 1995). During the past several decades, the terrestrial ecosystem has served as a sink of carbon due to an excess in carbon storage over respiration and other processes, such as fires, decomposition, and soil turnover, which release carbon back to the atmosphere (Tans et al. 1990; Gurney et al. 2002; Stephens et al. 2007). The net uptake of carbon by terrestrial ecosystems plays an important role in reducing the increase of atmospheric CO_2 concentrations. The factors controlling the net exchange of carbon by the terrestrial ecosystems is the focus of a number of ecosystem and atmospheric studies. The Fluxnet studies provide a network of sites to observe and to understand the factors affecting net carbon exchange in different biomes across the globe. This study utilizes the long term forest ecosystem observations of the Niwot Ridge Ameriflux site to explore the role of variable photosynthetic rates on seasonal carbon exchange in this ecosystem.

Movement of atmospheric and sub-surface nutrients into plants is critical for modeling any ecosystem. Atmospheric models tend to have relatively simple land surface sub-models that underestimate the importance of nutrient fluxes moving through the soil and ground water. Land surface models can oversimplify impacts of solar radiation and evapotranspiration, especially in areas that have a complex and variable climate. By

1

combining the soil subsurface model of DayCent (the daily version of the CENTURY model) and the photosynthetic sub-model of the SIPNET (Simple Photosynthesis and Evapotranspiration) model, we hope to achieve a robust model capable of representing the structure and processes of nutrient fluxes at a mid-elevation (3050 m asl) evergreen forest ecosystem.   The new version of the model is called DayCent-Photosyn to differentiate it from other versions in the CENTURY family of models.

Net ecosystem exchange (NEE) is the difference in carbon flux between gross primary production (GPP or total carbon uptake) and ecosystem respiration (Re), including both autotrophic (Ra) and heterotrophic respiration (Rh). To improve the GPP flux estimates, a photosynthetic sub-model was incorporated into the existing version of the DayCent model. The photosynthetic sub-model represents the total carbon uptake due to photosynthetic activity.

A key consideration, in this analysis, is the role of seasonal changes in the daily maximum photosynthetic rate (*Amax*) on GPP and ultimately the NEE flux estimates derived from GPP values. To account for variations in seasonal photosynthetic rates, modifications were made to the photosynthetic sub-model to incorporate a variable *Amax* term in the calculation of GPP. Variations in photosynthetic capacity are a well-documented phenomenon in forest ecology research (Bourdeau 1959; Helms 1965; Mohren and Vandeveen 1995; Marshall et al. 2001; Huxman et al. 2003; Wang and Barrett 2003; McGarvey et al. 2004; Weiskittel et al. 2006) and occurs on a diurnal and seasonal time frames.

The application of variable photosynthetic rates to an ecosystem model will not only improve in carbon flux estimates at the seasonal and annual level but will also

contribute to our understanding of ecosystem responses to different climatic and environmental conditions, such as drought and other environmental stresses through changes in photosynthetic uptake patterns.

DayCent, a daily version of the CENTURY ecosystem model, was developed to model soil trace gas fluxes such as N_2O, NO_x, CH_4, and CO_2 (Parton et al. 1998; Del Grosso et al. 2000; Parton et al. 2001). Plant physiology is simulated by assimilation, allocation, and exchange of water, carbon and other nutrients through various compartments of the system, with each compartment representing a different plant function (roots, branches, large wood, leaves). The current version of the DayCent model estimates GPP as a scalar value approximately twice that of the calculated net primary production (NPP). Where potential net primary production is a function of maximum potential production (P_{mx}), soil temperature (T_p), available water (M_p), and a self-shading factor (S_p) (Parton et al. 1993) as:

$$NPP_p = (\ P_{mx},\ T_p,\ M_p,\ S_p).$$

Potential production is then downwardly regulated by available nutrients to estimate actual NPP.

Analysis from the current DayCent model, at the Niwot Ridge Ameriflux LTER site, has shown reasonable correlation with total system carbon exchange at the yearly level, but model output has shown a two- to five-week lag in the critical spring time NEE uptake period when compared with observed eddy covariance data. Model results have also shown an over simplification of the complex inter-annual pattern and tend to overestimate carbon assimilation (uptake of carbon into the plant) throughout the growing season and under estimate carbon assimilation during the early growing season.

3

Research by Monson et al. (2005) has shown that CO_2 assimilation during the early snow melt period represents a significant component of NEE that contributes a large portion of net plant uptake for the year. Modifications to the model will help move the over assimilation bias of the entire growing season to the spring period providing a better representation of inter-annual pattern dynamics.

The development of a new process representation of a simplified photosynthesis model and associated plant and ecosystem respiration were incorporated into the DayCent-Photosyn model in order to test the hypothesis regarding the role of a variable Amax has on NEE estimates from the Niwot Ridge LTER high altitude forest site. The photosynthesis sub-model was adapted from the SIPNET model (Braswell et al. 2005; Sacks et al. 2006) used at the site.

In addition, model-data synthesis techniques used with the SIPNET model was also applied to estimate model parameters by use of an optimization algorithm. The algorithm is a variation of Markov Chain Monte Carlo (MCMC) which samples a posterior distribution of model errors and ties parameter estimates to the observed eddy covariance carbon fluxes. Research conducted at Niwot Ridge (Braswell et al. 2005; Sacks et al. 2006; Sacks et al. 2007; Moore et al. 2008; Zobitz et al. 2008) has shown that the use of an extended series of flux measurements combined with the model-data fusion technique can provide reasonably well constrained estimates of system carbon fluxes and underlying system parameters. The MCMC approach to parameter optimization allows simultaneous estimations of multiple parameters that are either difficult to measure, highly correlated to one other, or both. Model evaluation, for the optimization process and validation runs, will be done against a combined likelihood of NEE and GPP,

because optimization against NEE flux measurements only leads to poor fitting of GPP and R_e fluxes. Data for optimization will be from years 1999 to 2005, and model validation will be against the data that were withheld from the optimization process from 2006 to 2008.

The three sources of error for our model study are: 1) data, 2) parameter and 3) those in the model structure. Data errors and errors in parameter values should be the same for the original DayCent model and the new photosynthetic versions thus analysis will focus on the errors associated with the model structure that are addressed by the addition of the new photosynthetic sub-model. We will evaluate the original DayCent model (Base) and against a version which has the photosynthetic sub-model and a single *Amax* value (Single-Amax) and the new model (DayCent-Photosyn) which has the photosynthetic sub-model and a variable Amax rate. Other than parameters used in the photosynthetic submodel, all other parameters values were kept the same (where possible) and the differences between the three versions of the model will be the result of the effect of the photosynthetic sub-model and the variable *Amax* modification.

Limitations in computational power limit the ability to run the complete parameter optimization scheme as described in the SIPNET papers by (Braswell et al. 2005; Sacks et al. 2006; Sacks et al. 2007; Moore et al. 2008). However, a near optimal parameter set, suitable for doing a model comparison, was retrieved with the methodology set forth in this paper. By improving the representation of GPP, we hope to improve our estimates of the carbon flux budget for the Niwot Ridge area, and other ecosystems, have a better depiction of the physiological process that will make any climate, seasonal, or atmospheric patterns easier to detect.

Site Description

Data used in this study were from the Niwot Ridge (C1) Ameriflux site, a mid-elevation (3050 m), subalpine forest on the western side of the Continental Divide. The site is part of the Roosevelt National Forest, approximately 50 miles west of Boulder, Colorado (40.0329N Latitude; -105.5464W Longitude) in the Rocky Mountain Range. The dominant tree species in this area consist of subalpine fir (*Abies lasiocarpa*), Engelmann spruce (*Picea engelmannii*), and lodgepole pine (*Pinus contorta*). Tree stand age is approximately 100 years old and is a natural secondary growth, established following clear-cut logging from 1900 to 1910. The understory is sparse, with 25% average cover, and is composed of seedlings, Whortleberry (*Vaccinium myrtillus L.*), moss, and lichens. Soil is sandy due to rocky granite composition with a surface layer of ~6 cm of organic material. Mean annual temperature is 4° C (Monson et al. 2002) and approximately 65% of the 800 mm of annual precipitation accumulates as falling snow. High-elevation forests are of particular interest for carbon flux research because they account for a large portion of plant CO_2 uptake in the western United States (Schimel et al. 2002). Estimates for above ground biomass of carbon range from 11,500 to 24,000 g C m^{-2} (Monson 2010a), and the site is fixating carbon with a cumulative annual rate of NEE, ranging from 60-80 g C m^{-2} (Monson et al. 2002).

Data Description

For this study Level 4 flux were retrieved from the Ameriflux website (cdiac.ornl.gov) (Monson 2010a). Fluxes were calculated by the eddy covariance method

(Baldocchi et al. 1988; Baldocchi 2003). A detailed description of data collection is available in several papers (Monson et al. 2002; Turnipseed et al. 2002; Turnipseed et al. 2003; Turnipseed et al. 2004). For a comparison of model results, half hour fluxes for NEE, GPP, evapotranspiration (ET), and ecosystem respiration (R_e) were aggregated into daily values since our model runs at a daily time step. Estimates for R_e were calculated by the short-term temperature response of nighttime NEE fluxes (Reichstein et al. 2005), and GPP estimates were calculated as GPP = R_e - NEE. Because the estimates of GPP and Re are based on NEE observation, some degree of self-correlation exists between GPP and Re values so we will only optimize on GPP and NEE and not all three flux values. The retrieved Ameriflux values of NEE and GPP are consistent with the observed values (Arain and Restrepo-Coupe 2005; Monson et al. 2005; Monson 2010a) for this site. Additionally, the use of the two fluxes (i.e., GPP and NEE) for optimization greatly improves the model results for all flux estimates and keeps the parameters controlling photosynthesis from over-fitting the data and exceeding the literature-defined parameter boundaries. The GPP values from the Ameriflux data set are a calculated product and not directly measured; therefore, all references to Ameriflux GPP values will clearly be labeled as estimates and not as observations.

Four climate variables: 1) air temperature (Ta_f), 2) precipitation (Precip), 3) global filled radiation (Rg_f), and 4) vapor pressure deficit (VPD_f) are used to drive the photosynthetic sub-model. These climatic variables are used in the DayCent weather file. The weather file consists of daily minimum and maximum air temperatures, daily total precipitation, and average daytime VPD and solar radiation measurements. The two flux variables used for model evaluation and the optimization process are: 1) net ecosystem

exchange (NEE_or_fMDS), and 2) gross primary production (GPP_or_MDS). Flux data is gap-filled using the Marginal Distribution Sampling (MDS) method (Papale and Valentini 2003; Reichstein et al. 2005) and u-star filtered, to account for periods of low turbulence in the air mass that affect flux calibrations. The MDS method derives missing values by averaging values for data collected under similar meteorological conditions. Flux data from the Ameriflux web site is also available using Artificial Neural Network method (ANN) for gap-filling. Although ANN method has been shown to be marginally better than MDS (Moffat et al. 2007) for gap filling flux data on a cross site study, our study had better results using the MDS method (NEE & GPP log-likelihood of -1029.5) than with the ANN methodology (NEE & GPP log-likelihood of -1210.8) so we chose to use the MDS data gap-filling method.

MODEL AND METHODS

Parameter Optimization

The photosynthesis sub-model used to calculate GPP is from the SIPNET model (Monson et al. 2003; Braswell et al. 2005; Sacks et al. 2006; Sacks et al. 2007). The SIPNET model is based on the PnET model (Aber and Federer 1992) and was designed to be used with data from eddy flux towers in a model-data fusion approach for estimating parameter values. A key feature of the SIPNET model is its ability to run the model in two modes: 1) parameter optimization, and 2) forward, where the optimized parameter set is used to run the model. The DayCent-Photosyn model incorporates both the GPP sub-model from SIPNET and in addition uses the parameter optimization techniques to estimate the carbon fluxes at the Niwot Ridge site.

Parameter ranges and initial starting values that are directly equivalent to the parameters of the SIPNET model are used from the previous work of Moore and others (2008), see Table 1.

Table *1*. Photosynthetic parameters, starting values and ranges. Parameters marked with an (*) are taken from Moore et al. (2008). Values marked with a (#) are from Sarah Davis, personal communication. Estimates for *PS2Mrsp* are taken from literature values for maintenance respiration (Ryan and Waring 1992).. Fixed parameters do not change during the optimization process. Parameters are considered to have no units unless labeled otherwise.

Parameter	Description	Range	Starting Value
+*PS2Mrsp*	Fraction of GPP applied to maintenance respiration	0.3 to 0.65	0.46
Amax	Maximum net CO_2 assimilation rate	0 to 34	4.9 (g C m^{-2})
AmaxFrac	Ave. daily max photosynthesis as a fraction of *Amax*	fixed	0.76
AmaxScalar1	Scalar value of *Amax* at *GrowthDays1*	fixed	0
AmaxScalar2	Scalar value of *Amax* at *GrowthDays2*	0.8 to 1.6	1.22
AmaxScalar3	Scalar value of *Amax* at *GrowthDays3*	0.7 to 1.5	1.03
AmaxScalar4	Scalar value of *Amax* at *GrowthDays4*	0.3 to 0.8	0.6
Attenuation	Canopy Par extinction coefficient	fixed	0.5
BaseFolRespFrac	Foliar respiration as a fraction of *Amax*	0.05 to 0.3	0.06
CFracLeaf	Fraction of carbon applied to leaf growth	0.2 to 1	0.52
#*DVPDExp*	Exponent of VPD-photosynthesis relationship	fixed	-0.35
#*DVPDSlope*	Slope of VPD-photosynthesis relationship	fixed	1.55 (kPa^{-1})
GrowthDays1	First day of growth to apply *AmaxScalar1* scalar	fixed	1 (day)
GrowthDays2	Number of days after the start of growth to apply *AmaxScalar2* scalar	20 to 120	42 (days)
GrowthDays3	Number of days after the start of growth to apply *AmaxScalar3* scalar	121 to 180	136 (days)
GrowthDays4	Number of days after the start of growth to apply *AmaxScalar4* scalar	181 to 220	209 (days)
HalfSatPAR	Half saturation point of PPFD-photosynthesis relationship	4 to 12	8.3 (mol m^{-2} day^{-1})
LeafCSPWT	Carbon content of needles on a per-area basis	fixed	270
PsntMin	Minimum temperature for photosynthesis	-8 to 8	-3.5 (°C)
PsntOpt	Optimum temperature for photosynthesis	5 to 30	18.9 (°C)

The parameter optimization scheme used is a variation of the Metropolis-Hastings algorithm, with a simulated annealing algorithm (Hurtt and Armstrong 1996) to help prevent parameter values from settling into local optima. The algorithm performs a quasi-random walk through the parameter space, via the Metropolis-Hastings algorithm,

to find a parameter set that minimizes model error and maximizes the likelihood function

(*L*) (Braswell et al. 2005; Sacks et al. 2006; Sacks et al. 2007; Moore et al. 2008). The

maximum likelihood estimation (MLE) is the parameter vector that most strongly

supports the data (Fisher 1932). Maximum likelihood principal allows for several

candidate models (or model parameterizations in this case) to be evaluated and ranked

based on the support (how well they fit the data) (Johnson and Omland 2004).

Model optimization using likelihood provides a quantitative way to compare

model hypothesizes and allow us to calculate confidence bounds of parameters, which we

cannot do with sum of squares (Hilborn and Mangel 1997). The likelihood equation

$$L = \prod_{i=1}^{n} \frac{1}{\sqrt{2\pi\sigma}} e^{-(x_i - \mu_i)^2 / 2\sigma^2}$$

where *n* is the number of observations, σ is the standard deviation for the data, x_i is an

observed data point, and u_i is the corresponding modeled point.

The likelihood function is defined as a product, and log-likelihood is a sum, and

maximizing a product is more difficult than maximizing a sum. By using log-likelihood,

we are also able to sum probabilities for multiple parameters of interest, in this case, NEE

and GPP, for a total likelihood or *Ltotal*. By convention we are using a negative log-

likelihood, as seen in the following equation, since we are maximizing the likelihood

function and future references to log-likelihood should be considered a negative log-

likelihood. The best parameter set produces a result that maximizes log-likelihood which

is computed as:

$$l = -\left[n \log \sigma\right] - \left[\frac{1}{2\sigma^2} \sum_{i=1}^{n} (x_i - \mu_i)^2\right].$$

This form of the log-likelihood equation is easy to work with because the number of observations n and the sum of squares of the residuals is readily available, and the standard deviation can be estimated from the sum of squares. Constants that do not affect the likelihood comparison were removed from the equation. An estimate, σ_e, for the standard deviation, σ, is used because the actual error for NEE and GPP data is unknown. Using synthetic data sets, Braswell et al. (2005) found σ_e to be a suitable estimate for σ, calculated as:

$$\sigma_e = \sqrt{\frac{1}{n}\sum_{i=1}^{n}(x_i - \mu_i)^2}.$$

For each run (a 2,000 year simulation) in the optimization process a parameter is randomly selected and then changed by a random amount and is compared against observed NEE and estimated GPP data. If the new candidate parameter set increases log-likelihood, that set is then accepted. If the new candidate set does not have an improved likelihood, it may still be accepted with a probability equal to the difference of the log-likelihoods from the old to the new parameter sets to ensure that the global optimum is found. The likelihood calculation is an iterative Bayesian calculation sampled from a posterior distribution of the model error that is assumed to have a Gaussian probability distribution. After an adequate number of runs, the sampled space should represent the posterior probability distribution of parameters, and the Metropolis-Hastings algorithm guarantees convergence to a stationary point in the parameter space.

Seven independent model trials were run with same starting parameters (Table 2). The Heidelberger-Welch convergence diagnostic (Heidelberger and Welch 1981; Heidelberger and Welch 1983) was run from the R CODA package (heidel.diag) to test each trial for convergence ($\epsilon = 0.1$ pvalue$= 0.05$). The diagnostic consists of two parts: a

stationary portion test and a half-width test. The stationary test uses the Cramer-von-Mises statistic to test the null hypothesis that the sampled values come from a stationary distribution. If the null hypothesis is rejected the test is repeated discarding the first 10% of the iterations. If the null hypothesis is rejected another 10% of iterations are discarded. The stationary test continues until either the test is passed or 50% of the iterations are used, resulting in a test failure.

The half-width test calculates a 95% confidence interval for the mean, using the iterations that had passed the stationary test. This tests the accuracy for the mean estimates. Seven model trials of 10,000 iterations (Fig. 1) were run for both models and all passed the Heidelberger-Welch stationary test. Result for the Photosyn model, (mean P-value =0.54) and half-width test (mean log-likelihood = -1055.4, mean half-width = 10.48). Single-Amax model Heidelberger-Welch stationary test (mean P-value =0.591) and half-width test (mean log-likelihood = -1366, mean half-width = 9.92).
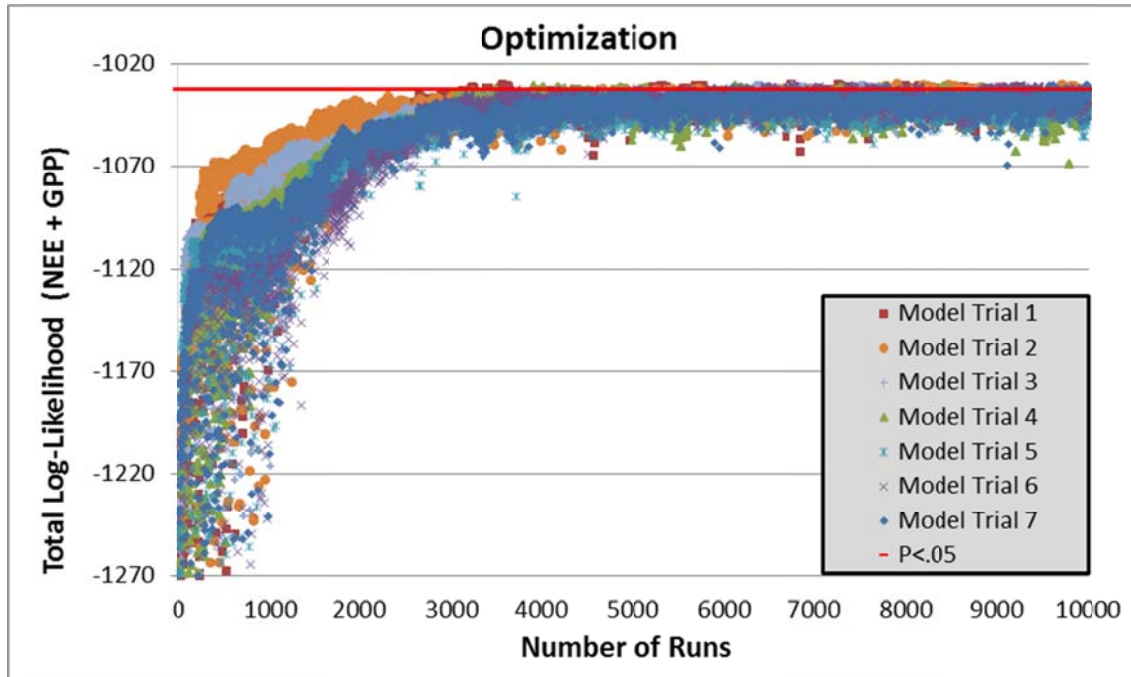
Fig. 1 Log-likelihood for the seven model trials of the DayCent-Photosyn model. Results of model run on and above the red line are statistically similar (P = .05) to the best overall model run in terms of likelihood (-1029.5). Note that convergence of likelihoods begins at 3,000 to 4,000 model iterations for each trial.

12

While Heidelberger-Welch convergence diagnostic is not a guarantee that the global optima has been reached, it is a good indication that we have reached a stationary process and that further iterations are not needed for an acceptable, if not the best, parameter set. A further sensitivity analysis was run on the best retrieved parameterization set from each of the seven trials (DayCent-Photosyn *Ltotal* ranging from -1029.5 to -1031.1 and Single-Amax ranging from -1850.0 to -1852.1) and no statistically better parameterization ($\alpha = 99\%$) was found.

Extra parameters, associated with more complex models, increases the degrees of freedom for the model and my lead to better log-likelihood values by overfitting the data and not improving model performance. Akaike's Information Criterion (AIC) (Akaike 1974) is a tool for model selection and provides a measure of goodness of fit. The AIC index quantifies the differences between observed data and modeled output by maximizing the likelihood-ratio [$\ln(L)$] and assesses a penalty for each additional parameter a model has over competing models using the same data set. The penalty is a way to control overfitting data by discouraging inclusion of additional parameters for relatively small gains in model fit.

$$AIC = 2\,k - 2\,\ln(L)$$

where k is the number of parameters and $\ln(L)$ is equal to the log-likelihood for each model. AIC values will be computed, along with log-likelihood, to account differences in the number of parameters for each model.

Photosynthetic Model Changes

We incorporated the SIPNET photosynthesis routine into DayCent to calculate estimates for GPP. GPP is calculated as a function of *Amax* and climatic parameters and then added to the stored carbohydrate pool where the CO_2 is released in the form of maintenance respiration. The remaining reserves are available for the NPP (Fig. 2). To determine GPP, a maximum photosynthetic assimilation rate (GPP_{max}) is calculated as the unstressed (not including climatic factors) net instantaneous CO_2 assimilation rate per unit leaf mass:

$$GPP_{max} = Amax * (AmaxFrac + BaseFolRespFrac)$$
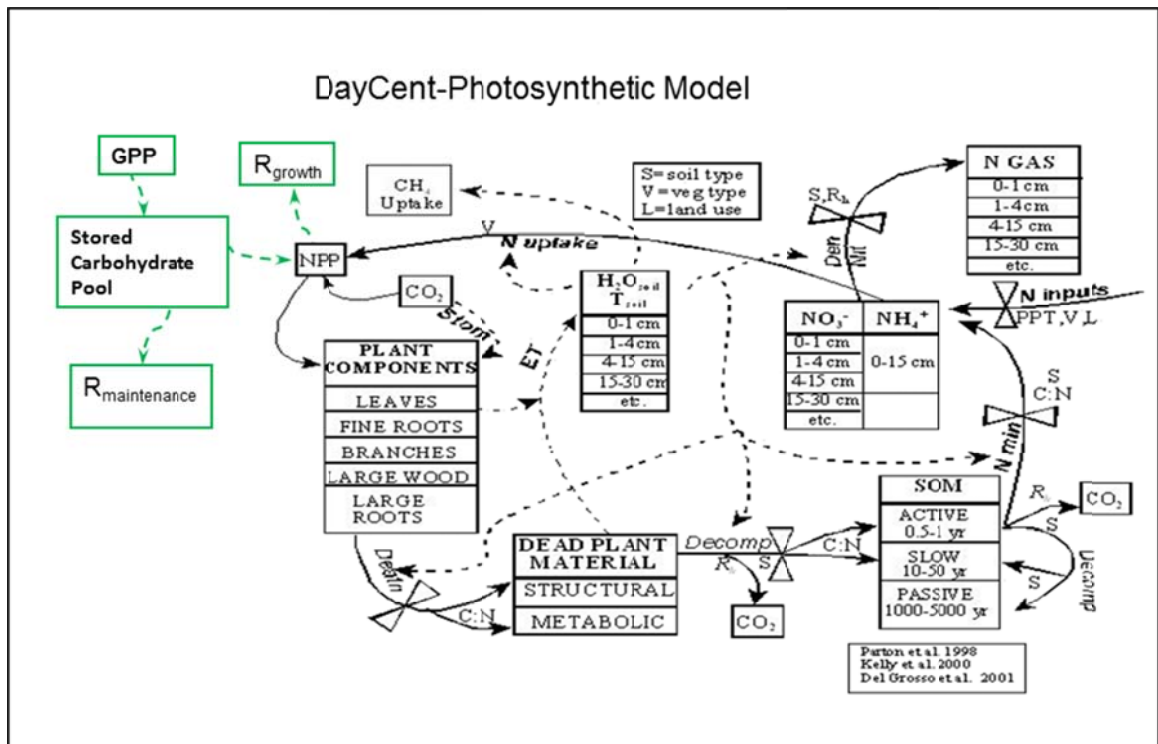
Fig. 2 The DayCent model with the photosynthetic modifications in green. Maintenance respiration is based on the *PS2Mrsp* parameter.

Maximum gross photosynthesis is then scaled by the four terms that represent climatic conditions with values between 0 and 1: 1) temperature (D_{temp}), 2) vapor pressure deficit

(D_{vpd}), 3) solar radiation (D_{light}), and 4) a water stress term (D_{water}) shown as:

$$GPP = GPP_{max} * D_{temp} * D_{vpd} * D_{light} * D_{water}$$

A detailed description and equation for these scaling terms can be found in previous work by Braswell and others.

The calculation for D_{vpd} was modified to improve the effect of stomatal conductance due to lack of air moisture (VPD), expressed as an exponential decline in efficiency (Drake et al. 2010):

$$D_{vpd} = DVPDSlope \ \ e^{\ (DVPDExp * VPD)}$$

Photosynthesis is downwardly regulated during the growing season when the minimum air temperature approaches 0° C based on a relationship between stomatal conductance, temperature, and photosynthesis (Kaufmann 1982; Moore et al. 2008). Where *T* is the daily average temperature:

$$GPP_{scalar} = .4 + .075 \ (6 + T)$$

Seasonal Amax dynamics were developed to capture the higher peak uptake during the spring and the lower photosynthetic rates observed in the fall. Four factors that contribute to a variable maximum assimilation rate are: 1) an initial lower starting value due to slow recovery of stomatal conductance (Monson 2005); 2) a negative response in carbon uptake due to increased temperature (Huxman et al. 2003); 3) differences in assimilation rates of young versus old needles as a result of biological function (Mohren and Vandeveen 1995; Marshall et al. 2001; McGarvey et al. 2004; Weiskittel et al. 2006); and 4) leaf area index (Wang and Barrett 2003) resulting from needle growth during the growing season. The seasonal variation in maximum net photosynthetic rates was implemented as a linear *Amax* response function. A similar type of response was seen in a study done by Marshall (2001) on Douglas-fir, Ponderosa pine,

and Western white pine in northern Idaho. The function scales the value of *Amax* from the start of one growth period to the start of the next, as defined by the *GrowthDays* parameters (the number of days since the start of the growing season) and scaled by the *AmaxScaler* parameters,

$$AmaxScaler = (GDays - GrowthDays1) \frac{AmaxScaler2 - AmaxScalar1}{GrowthDays2 - GrowthDays1} + AmaxScaler1$$

The function as it appears from the start of growth, *GrowthDays1*, until *GrowthDays2*, where *GDays* is the number of days since the start of growth. The function allows the primary *Amax* value to be scaled three times during the growing season, from late April to early November. The AmaxScalar function is original the range and starting values for the *AmaxScalar* and *GrowthDays* parameters were unknown. In order to set reasonable range and starting values for these parameters we used a long iteration (10,000) optimization run with the parameters boundaries set at their maximum expected values (*AmaxScalar* 0 to 3 and *GrowthDays* 0- 230). After analysis of the results we set the range for each parameter to be a least three times the standard deviation, except in cases where the parameter would be going over parameter boundaries, and the initial starting values were set to be mean values from the optimization process.

Model Comparison Experiment

The focus of this paper is to evaluate the effect of variable photosynthetic rates on system carbon uptake by analyzing model results of the DayCent model with a photosynthetic submodel and variable *Amax* parameterization. The simulations results and observation data provide the information necessary to evaluate the relationship between variable photosynthetic capacity and NEE compared to a linear *Amax*

approximation. The modeling study and analysis of observational data provides information to evaluate the biological pattern associated with variable photosynthetic rates in this ecosystem across multiple seasons.

The DayCent Base version will be included in the comparison of NEE values because it will help us illustrate the redistribution of plant carbon uptake in the early season using the photosynthetic versions and provides a baseline for annual NEE values. We will not include GPP results for the Base model because they are only an approximation of GPP and will provide no real data about model improvements in GPP estimates. The Base version also does not include many other small changes in the model so any comparison with the photosynthetic versions of the DayCent model would not provide us with additional information about variable photosynthetic capacity.

The Single-Amax version will incorporate the photosynthetic submodel and the parameter optimization routine will treat *Amax* as a single value for the entire growing season. This will become our baseline of comparison for the effect of variable photosynthetic capacity on GPP and NEE.

The DayCent-Photosyn version incorporates the photosynthetic submodel and the parameter optimization routine will allow the Amax rate to vary four times during the growing season. The initial starting value for variable Amax parameters will be 0% percent and will linearly increase until the Amax parameter reaches its max on day 44 of the growing season at 1.27% of the Amax parameter. The Amax scalar will gradually decrease to 1.17% by day 135 and then rapidly decrease to .38% toward the end of the growing season on day 211.

Model comparison will be done on the best parameterization set found for each of the photosynthetic versions of the model. The version that yields the highest log-likelihood (the smallest negative number) indicates the model has a better fit with the data. In addition to looking modeling metrics we will also look that season flux patterns to justify model changes and effects of variable photosynthetic capacity. Model validation, using withheld data, will be limited to the DayCent-Photosyn model version because of the photosynthetic sub-model will be identical for each model and parameter optimization results for each version are statically similar.

RESULTS

Optimization Results

The best retrieved parameter values (Table 2), were significantly different from the original starting parameter used from Moore et al. (2008). We expected to see differences in the parameterizations because the DayCent-Photosyn model optimized on two carbon flux values, (NEE and GPP), and the SIPNET model used NEE and ET.

We chose not to use ET as an optimization parameter because changes in photosynthetic parameters do not affect the value of ET in our version of the photosynthetic sub-model.

Values of the best parameterizations fell well within the allowable range for each parameter for both models. However, values for *BaseFolRespFrac* and *HalfSatPAR* were "edge-hitting," i.e. retrieving values that were close to their range limits. The mean and standard deviation of parameter sets (Table 2) that are statistically similar (P = 0.05) to the best model parameterization for DayCent-Photosyn and Single-Amax model were

calculated. The means of almost all parameters were within one standard deviation of the best parameter set's values. The one exception was *BaseFolRespFrac* parameter for the DayCent-Photosyn model which had a different mean but was within two standard deviations. The *BaseFolRespFrac* parameter contributes less than 8% to the base value of potential GPP and even at two standard deviations the parameter uncertainty does not have a significant effect on model results >5%.

Table 2.   Parameters marked with (#) are fixed and do not vary during optimization. The values from the best parameter set are in bold. The numbers beside the best parameter set are parameterizations from the runs that that were statistically similar (P = 0.05) in terms of likelihood. With the first number being the mean and the number after (±) being the standard deviation of the mean.

Parameter	Single-Amax Values	DayCent-Photosyn Values
PS2Mrsp	**0.50** (0.48 ± .03)	**0.44** (0.45 ± .02)
Amax	**3.63** (3.83 ± .34)	**3.76** (3.79 ± .22)
#AmaxFrac	**0.76**	**0.76**
#AmaxScalar1	**1.0**	**0.0**
AmaxScalar2	**1.0**	**1.27** (1.27 ± .04)
AmaxScalar3	**1.0**	**1.17** (1.16 ± .04)
AmaxScalar4	**1.0**	**0.38** (0.4 ± .02)
#Attenuation	**0.5**	**0.5**
BaseFolRespFrac	**0.100** (0.112 ± 0.021)	**0.055** (0.095 ± 0.027)
CFracLeaf	**0.56** (0.58 ± 0.04)	**0.59** (0.62 ± 0.03)
#DVPDExp	**-.35**	**-.35**
#DVPDSlope	**1.55**	**1.55**
#GrowthDays1	**1**	**1**
GrowthDays2	**1**	**44** (44 ± 0.48)
GrowthDays3	**1**	**135** (135 ± 1.22)
GrowthDays4	**1**	**211** (210 ± 2.00)
HalfSatPAR	**4.02** (4.21 ± 0.19)	**4.25** (4.25 ± 0.14)
#LeafCSPWT	**270.0**	**270.0**
PsntMin	**-1.51** (-1.69 ± 0.54)	**-6.67** (-6.23 ± 0.60)
PsntOpt	**15.68** (15.85 ± 0.28)	**11.67** (11.68 ± 0.14)

However one should be aware that while the contribution of foliar respiration to total GPP is small for coniferous ecosystem, it may contribute more to other ecosystems, such as a deciduous forest, where foliar respiration constitutes a greater portion of GPP. Photosynthetic capacity and foliar respiration are positively correlated (Ceulemans and

Saugier 1991) and coniferous trees generally have lower photosynthetic capacity then deciduous trees (Sprugel et al. 1995).

Model Comparison Results

In a comparison between observed and modeled NEE the Single-Amax (RMSE of 0.74 g C m^{-2}) and DayCent-Photosyn (RMSE of 0.63 g C m^{-2}) models both show improvement over the Base model with the DayCent-Photosyn version having the best results (Table 3). These models improved accuracy of NEE estimates over the Base model by 12% and 25% respectively. GPP model error for the DayCent-Photosyn version (RMSE of 0.88 g C m^{-2}) was also about 14% better than the Single-Amax version (RMSE of 1.02 g C m^{-2}).
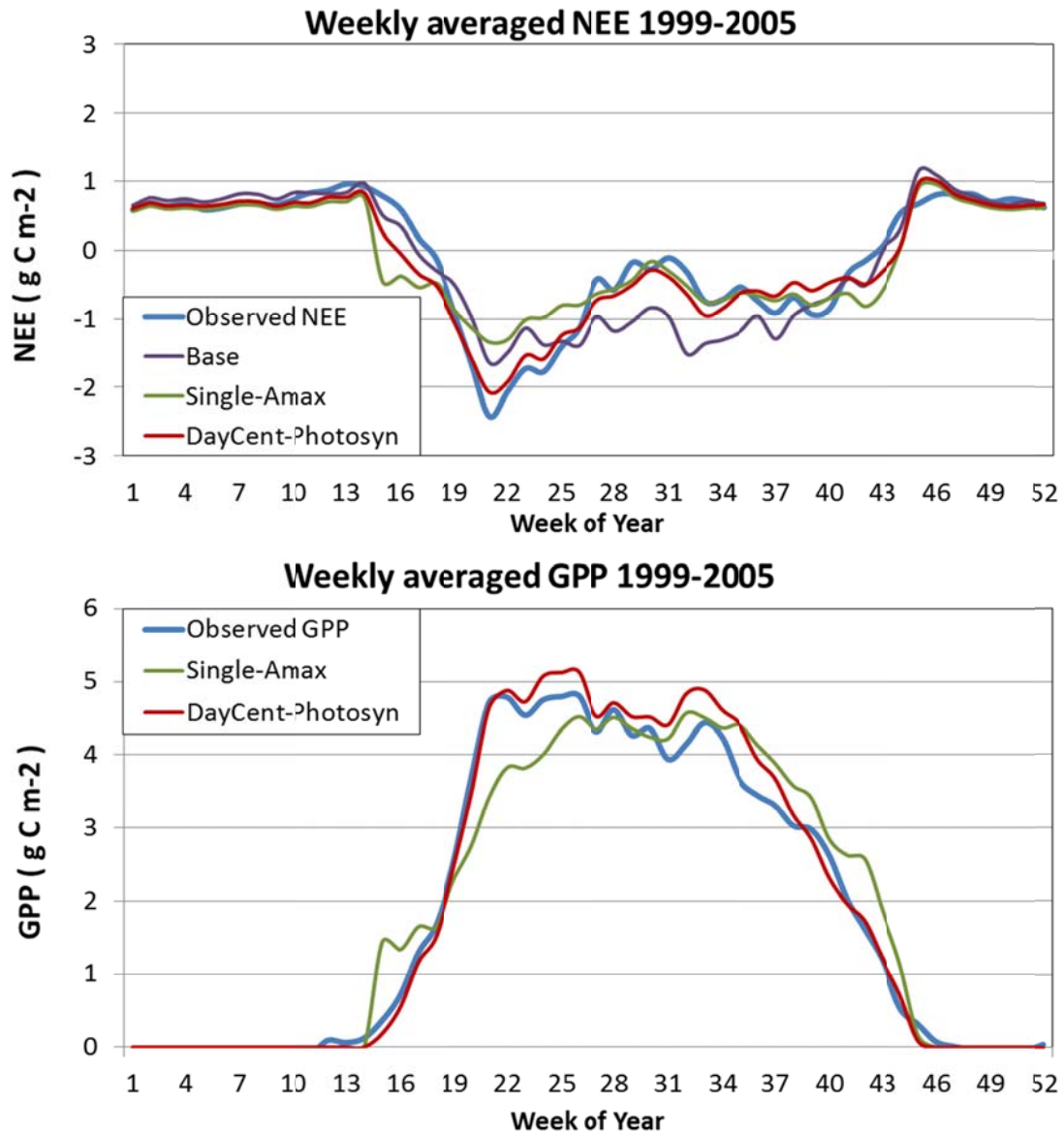
Table 3. Model comparison for DayCent model. Note that no GPP data are available for the Base model (*). Single-Amax is the photosynthetic version of DayCent with a single *Amax* value. DayCent-Photosyn is the photosynthetic model with seasonal variation of *Amax*. Root Mean Square Error (RMSE) is a measure of the amount of variance not explained by the model, lower is better. Akaike Information Criterion (AIC) equation is *2K – 2ln(L)*, where *ln(L) = Ltotal*. A lower AIC indicates the model that has better support from the data.

DayCent Model	Base*	Single-Amax	DayCent-Photosyn
Log-likelihood (*Ltotal*)	Na	-1850.0	-1029.5
NEE RMSE (gC m^{-2})	0.84	0.74	0.63
NEE R^2	0.57	0.57	0.69
GPP RMSE (gC m^{-2})	Na	1.02	0.88
GPP R^2	Na	0.78	0.84
Number of Parameters (*K*)	0	12	20
AIC	Na	3723.9	2099.0

The DayCent-Photosyn model out performed both other models in calculating NEE and GPP values (Table 3) in all the relevant statistics with a greater percentage of the model variation better explained by the model (NEE R^2 = 0.69, GPP R^2= 0.84) and an increased log-likelihood (-1029.5). The increase in model performance by the DayCent-Photosyn model over the Base and Single-Amax models are the result of including the photosynthetic sub-model and use of a variable *Amax*. AIC values are

calculated to account for differences in the number of parameters in the different models. AIC values for the DayCent-Photosyn (AIC= 2099.0) model are significant better than for the Single-Amax model (AIC= 3723.9) and provide a better fit of the data better even when the penalty for the extra parameters are taken into account (Table 3).

The average pattern of observed NEE at the Niwot Ridge site shows a strong downward pattern (uptake of carbon) in the early spring snow melt period (Fig 3).

Fig. 3. Model comparison of GPP and NEE for the optimization period from 1999-2005. The data is averaged into 52 weekly periods. Note there is no GPP data for the Base DayCent model.

This is followed by a reduction of uptake in mid-summer, as heterotrophic respiration increase, followed by another smaller increase in the latter summer period that coincides with summer monsoonal moisture common in this study area. In comparison the Base weakly follows this uptake pattern but is rather flat and over estimates carbon uptake model during the peak growing season, weeks 25-37. The Single-Amax and DayCent-Photosyn version are both able to pick-up the carbon assimilation patterns much better, but the Single-Amax version over estimates early season and under estimates peak NEE uptake.

Examination of NEE residuals between weeks 13-25 show over twice the cumulative error for the Single-Amax model (7.6 g C m^{-2}) when compared with the DayCent-Photosyn version (3.4 g C m^{-2}). Residual errors for the remainder of the growing season on are about the same at 2.5 and 2.9 g C m^{-2} respectively. Heterotrophic respiration, which is proportional to the amount of carbon in the system, is about the same because both models having a similar total system carbon between 1530 and 1540 g. This leaves error in predicting the GPP term as the major source of difference between the two photosynthetic models.

The optimization process produced similar parameter values for both versions of the photosynthetic model except for *BaseFolRespFrac, PsntMin* and *PsntOpt*. The *BaseFolRespFrac* parameter only controls a small portion of the amplitude of signal (moving the NEE output up or down) leaving *PsntMin* and *PsntOpt* and the variable Amax parameters the main difference in model output. The parameters *PsntMin, PsntOpt* control the D_{temp} term which scales GPP max term in following the equation.

$$Dtemp = \text{Max}\left(\frac{(Tmax - Tair) - (Tair - Tmin)}{(Topt - Tmin)^2}, 0\right)$$

Where T_{max} was calculated as T_{opt} + (T_{opt} − T_{min}).   The effect of temperature on photosynthesis is assumed to be a parabolic function and both model show almost identical responses curves. The main difference is the DayCent-Photosyn response starts much earlier and at a higher scalar value (Fig 4). The net effect on GPP is a quicker and larger response to early season temperature increases.
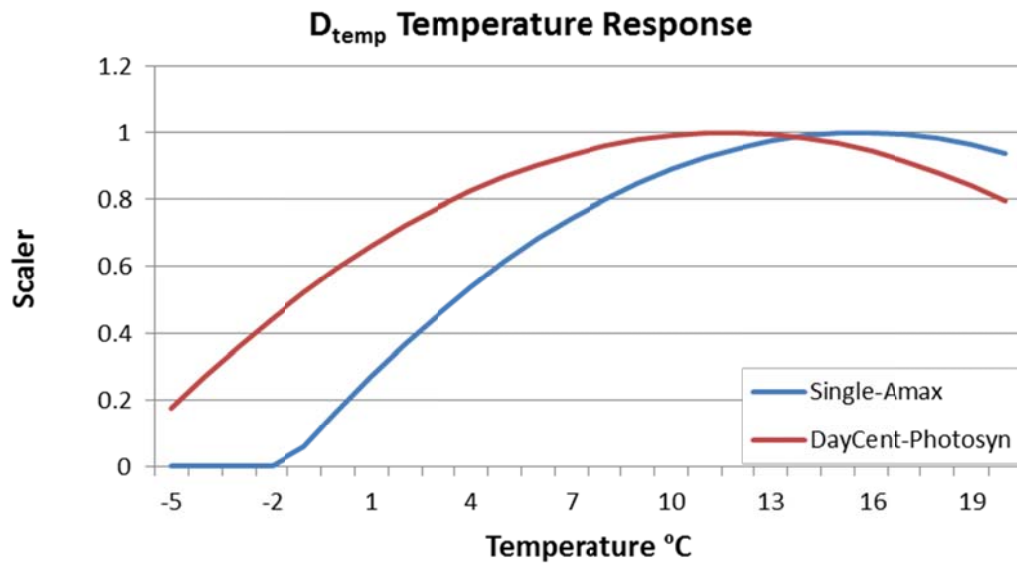
Fig. 4.   D*temp* temperature response curves. DayCent-Photosyn *PsntMin -6.67 ºC* and *PsntOpt 11.67 ºC*. Single-Amax Photosyn *PsntMin -1.51 ºC* and *PsntOpt 15.68 ºC*.

Because both models had the freedom to modify the *PsntMin* and *PsntOpt* parameters within the same range we can contribute the increase predicting in GPP and NEE estimates to the Amax variable parameters.

DayCent-Photosyn Model Validation

Model validation is done with GPP and NEE data withheld from the optimization period from 2006 to 2008, except estimates of GPP were not available for 2008. Validation runs for the DayCent-Photosyn model were done using the best parameter set

from the optimization process. A comparison for the optimization and validation period (Fig. 4) shows similar R^2 values for GPP and NEE estimates.

The pattern of results around the 1:1 line for NEE and GPP shows little bias in terms of over or under estimating fluxes, except for one year of GPP data during the optimization period.
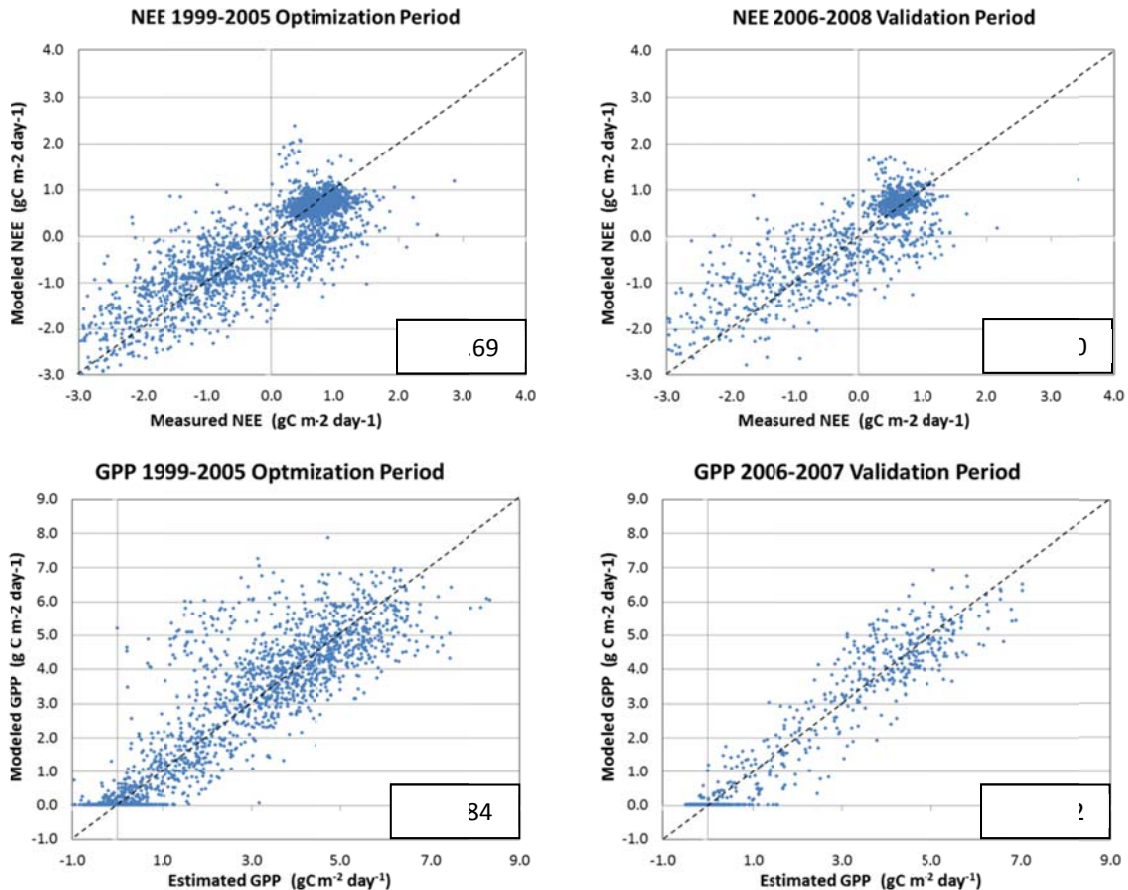

Fig. 5 Model versus data comparisons for the optimization period 1999-2005 and validation period 2006-2008. GPP data is not available for 2008. Positive NEE number denotes release of carbon from the ecosystem to the atmosphere. The large number of data points above one-to-one line for the GPP optimization period is a result of a large drop in summer time GPP from the observed data in the summer of 2004. If this data is removed, there is a much better correlation ($R^2 = 0.91$) with the validation period GPP.

The Ameriflux GPP data for 2004 has a large drop-off after the initial spring period which seems to be inconsistent with the other years of data and accounts for the greater difference seen in GPP R^2 values for the optimization period versus validation period

(Fig. 5). The difference in the 2004 GPP flux could be a result of either irregular climatic conditions or in the estimation techniques for GPP. However, since the flux is a dramatic departure from the typical observed pattern, we have included an R^2 value that excludes 2004 data in Figure 5.

An examination of NEE fluxes at a seasonal level shows a reasonable correspondence with observed data, yet there are some small differences in the flux patterns that result in a long-term overestimation of net carbon uptake (Fig. 6). The model tends to modestly, yet consistently, underestimates winter and mid-summer respiration rates. One would expect that these underestimated respiration rates would balance the lower uptake observed early in the spring, but annual NEE uptake values are almost always larger than the observed values when examined at an annual period.
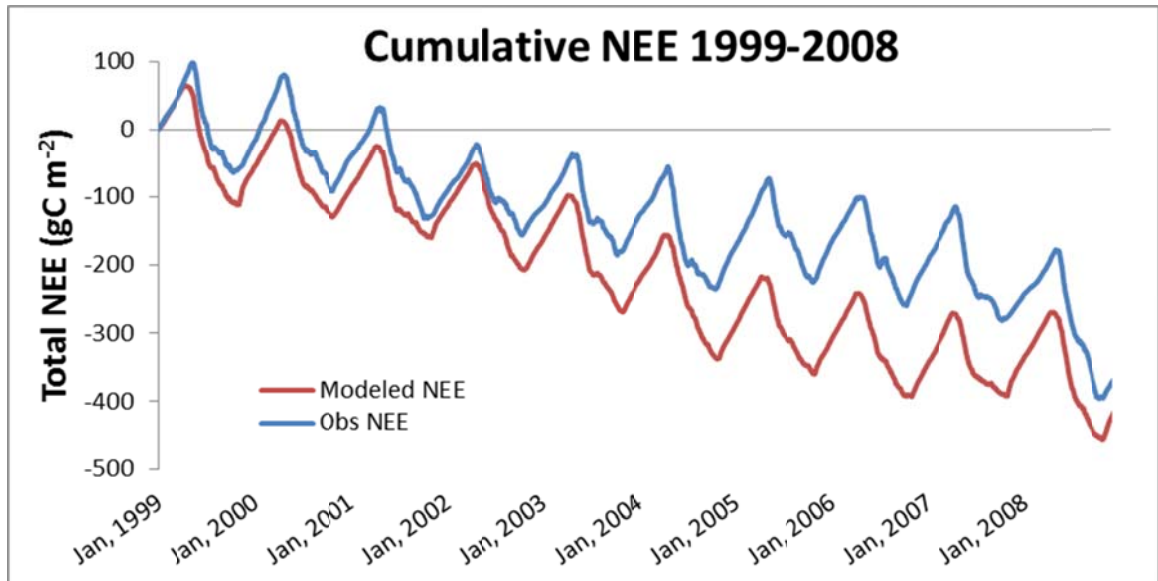
Fig. 6 Cumulative NEE comparison. NEE values on December 31, 2002 (modeled: -165.4; observed: -115.9), and on December 31, 2008 (modeled: -405.1; Observed: -359.1)

The DayCent-Photosyn model results correlate well with observed GPP (Fig. 6) so the additional NEE uptake is likely an underestimation of respiration at the outset of growth and during the late summer and early fall period.

The large inter-seasonal variation in the NEE and GPP fluxes for the Niwot Ridge site, combined with the additional parameters for the DayCent-Photosyn model, could lead to over-fitting the model to the data. A statistically different result in the validation period could be used to assess that concern. The similar NEE and GPP results obtained (Fig. 5) for the optimization and validation period strongly support the addition of not only the photosynthetic sub-model, but also the inclusion of the seasonally adjusted *Amax* parameters. When the 2004 GPP data are excluded from the results, the model is able to explain over 90% of the observed variation for the optimization and validation period and the NEE flux estimates were able to account for about 70% of model variation.

Discussion

Our results demonstrate the benefit of incorporating a photosynthetic sub-model into the DayCent model. Estimates for NEE, GPP, and respiration were much improved over results shown in the Base and even the Single-Amax models. However, carbon fluxes represent only a small portion of the total ecosystem processes that are simulated by the DayCent model. This study is only a start for validating the other accompanying sub-models and the ecosystems used with this model. Because of the complexity and large number of parameters available in the DayCent model, we limited our adjustments to only the new parameters added via the new sub-model. Certain issues in model performance could be addressed by adjusting other model parameters, such as autotrophic and heterotrophic respiration rates. The sub-model is also only loosely tied into the core DayCent processes through the carbohydrate storage pool. This was done purposefully as to not disrupt the current structure that has been tested and validated on a number of ecosystems. As the DayCent-Photosyn model is validated against more sites there will be

an opportunity to integrate the carbon cycle of the photosynthetic sub-model to other core system fluxes.

The parameter estimates retrieved from the optimization process worked far better than our initial estimates, and we were able to achieve converge in a relatively short time scale. Even though our final parameters differed from the initial starting parameters, the process benefited from using the starting values that were pre-optimized. Certain parameters are highly correlated, and their levels were balanced and set by the previous optimization runs done by Moore (2008). Using the pre-optimized parameters also reduced the range which the optimization process had to investigate since our starting values were closer to their final optimized values. Future optimization runs at sites without the extensive initial parameter information will likely result in much longer model runs required for model convergence.

The incorporation of seasonally adjusted *Amax* parameters lead to the largest improvement in our flux estimates of GPP, NEE and R_e. Because the high predictive capability of GPP future versions of the model should look at autotrophic respiration for further improvements in flux estimates. The biology behind the *Amax* function is certainly more complex than the linear function that we used and this should definitely be an area of further exploration.

Conclusion

For this study we modified the existing photosynthetic sub-model for the DayCent model. A comparison with the existing model shows strong support for inclusion of a photosynthetic sub-model with variable photosynthetic assimilation rates at biological

level, as a photosynthetic response to temperature. The real biological process behind the response involves the complex biology of stomatal conductance, enzymes and respiration that were not part of this study. And as a scientific hypothesis our aim is steer people into further research rather than guide them into the process of including of any addition functions.

Our research also included a model-data optimization process that links parameter values to observed data. The optimization process should not be underestimated in the effect that it had on model results. Our model results are for one site only, but with the multitude of eddy-covariance towers collecting long term flux records there is a great opportunity to not only refine the photosynthetic sub-model but also the optimization techniques used with large models.

Studies of carbon sequestration tend to focus on only one value, NEE, but because of the complex input and output the DayCent model provides we can look at carbon sequestration in terms of smaller units such as roots and branches which maybe more important from an ecosystem perspective. This can help answer the why and how rather than just the how much questions that exist with carbon sequestration. By modeling the seasonal variation in the NEE flux pattern we were able to extracting information about the necessary model structure needed to simulate the biological function of photosynthesis. Extrapolating model structure to a biological process equation will be the next significant step in understanding the effect of Amax for different ecosystems. Once this is in place we can gain a further understanding the on the role variable Amax plays on ecosystems under various levels of stress.

BIBLIOGRAPHY

Aber, J. D. and C. A. Federer (1992). "A generalized, lumped-parameter model of photosynthesis, evapotranspiration and net primary production in temperate and boreal forest ecosystems." Oecologia **92**(4): 463-474.

Akaike, H. (1974). "New look at statistical-model identification." Ieee Transactions on Automatic Control **AC19**(6): 716-723.

Arain, A. A. and N. Restrepo-Coupe (2005). "Net ecosystem production in a temperate pine plantation in southeastern Canada." Agricultural and Forest Meteorology **128**(3-4): 223-241.

Baldocchi, D. D. (2003). "Assessing the eddy covariance technique for evaluating carbon dioxide exchange rates of ecosystems: past, present and future." Global Change Biology **9**(4): 479-492.

Baldocchi, D. D., B. B. Hicks and T. P. Meyers (1988). "Measuring biosphere-atmosphere exchanges of biologically related gases with micrometeorological methods." Ecology **69**(5): 1331-1340.

Bourdeau, P. F. (1959). "Seasonal bariations of the photosynthetic efficiency of evergreen conifers." Ecology **40**(1): 63-67

Braswell, B. H., W. J. Sacks, E. Linder and D. S. Schimel (2005). "Estimating diurnal to annual ecosystem parameters by synthesis of a carbon flux model with eddy covariance net ecosystem exchange observations." Global Change Biology **11**(2): 335-355.

Ceulemans, R. and B. Saugier (1991). Photosynthesis: Physiology of Trees. New York, John Wiley & Sons.

Del Grosso, S. J., W. J. Parton, A. R. Mosier, D. S. Ojima, A. E. Kulmala and S. Phongpan (2000). "General model for N2O and N-2 gas emissions from soils due to dentrification." Global Biogeochemical Cycles **14**(4): 1045-1060.

Drake, J. E., L. M. Raetz, S. C. Davis and E. H. DeLucia (2010). "Hydraulic limitation not declining nitrogen availability causes the age-related photosynthetic decline in loblolly pine (Pinus taeda L.)." Plant Cell and Environment **33**(10): 1756-1766.

Fisher, R. A. (1932). "Inverse Probability and the Use of Likelihood." Proceedings of the Cambridge Philosophical Society **28**: 257-261.

Gurney, K. R., R. M. Law, A. S. Denning, P. J. Rayner, D. Baker, P. Bousquet, L. Bruhwiler, Y. H. Chen, P. Ciais, S. Fan, I. Y. Fung, M. Gloor, M. Heimann, K. Higuchi, J. John, T. Maki, S. Maksyutov, K. Masarie, P. Peylin, M. Prather, B. C. Pak, J. Randerson, J. Sarmiento, S. Taguchi, T. Takahashi and C. W. Yuen (2002). "Towards robust regional estimates of CO2 sources and sinks using atmospheric transport models." Nature **415**(6872): 626-630.

Heidelberger, P. and P. D. Welch (1981). "A spectral method for confidence interval generation and run length control in simulations." Communications of the ACM **24**(no. 4): 233-245.

Heidelberger, P. and P. D. Welch (1983). "Simulation run length control in the presence of an initial transient." Operations Research: 1109-1144.

Helms, J. A. (1965). "Diurnal and Seasonal Patterns of Net Assimilation in Douglas-Fir, Pseudotsuga Menziesii (Mirb). Franco, as Influenced by Environment." Ecology **46**(5): 698-708.

Hilborn, R. and M. Mangel (1997). The ecological detective: confronting models with data. , Princeton University Press, Princeton NJ.

Hurtt, G. C. and R. A. Armstrong (1996). "A pelagic ecosystem model calibrated with BATS data." Deep-Sea Research Part Ii-Topical Studies in Oceanography **43**(2-3): 653-683.

Huxman, T. E., A. A. Turnipseed, J. P. Sparks, P. C. Harley and R. K. Monson (2003). "Temperature as a control over ecosystem CO2 fluxes in a high-elevation, subalpine forest." Oecologia **134**(4): 537-546.

Johnson, J. B. and K. S. Omland (2004). "Model selection in ecology and evolution." Trends in Ecology & Evolution **19**(2): 101-108.

Kaufmann, M. R. (1982). "Evaluation of season, temperature, and water-stress effects on stomata using a leaf conductance model." Plant Physiology **69**(5): 1023-1026.

Marshall, J. D., G. E. Rehfeldt and R. A. Monserud (2001). "Family differences in height growth and photosynthetic traits in three conifers." Tree Physiology **21**(11): 727-734.

McGarvey, R. C., T. A. Martin and T. L. White (2004). "Integrating within-crown variation in net photosynthesis in loblolly and slash pine families." Tree Physiology **24**(11): 1209-1220.

Moffat, A. M., D. Papale, M. Reichstein, D. Y. Hollinger, A. D. Richardson, A. G. Barr, C. Beckstein, B. H. Braswell, G. Churkina, A. R. Desai, E. Falge, J. H. Gove, M. Heimann, D. Hui, A. J. Jarvis, J. Kattge, A. Noormets and V. J. Stauch (2007). "Comprehensive comparison of gap-filling techniques for eddy covariance net carbon fluxes." Agricultural and Forest Meteorology **147**(3-4): 209-232.

Mohren, G. M. J. and J. R. Vandeveen (1995). "Forest growth in relation to site conditions, applicaiton of the model FORGRO to the solling spruce site." Ecological Modelling **83**(1-2): 173-183.

Monson, R. K. (2010a). " US-NR1 site description, Ameriflux Niwot Rige, Oak Ridge Natl. Lab., Oak Ridge, Tenn." from http://public.ornl.gov/ameriflux/.

Monson, R. K., W. Sacks, J., A. A. Turnipseed, S. Burns and D. S. Schimel (2003). "A Bayesian model-data fusion analysis of net ecosystem CO2 exchange in a high-elevation, subalpine forest."

Monson, R. K., J. P. Sparks, T. N. Rosenstiel, L. E. Scott-Denton, T. E. Huxman, P. C. Harley, A. A. Turnipseed, S. P. Burns, B. Backlund and J. Hu (2005). "Climatic influences on net ecosystem CO2 exchange during the transition from wintertime carbon source to springtime carbon sink in a high-elevation, subalpine forest." Oecologia **146**(1): 130-147.

Monson, R. K., A. A. Turnipseed, J. P. Sparks, P. C. Harley, L. E. Scott-Denton, K. Sparks and T. E. Huxman (2002). "Carbon sequestration in a high-elevation, subalpine forest." Global Change Biology **8**(5): 459-478.

Moore, D. J. P., J. Hu, W. J. Sacks, D. S. Schimel and R. K. Monson (2008). "Estimating transpiration and the sensitivity of carbon uptake to water availability in a subalpine forest using a simple ecosystem process model informed by measured net CO2 and H2O fluxes." Agricultural and Forest Meteorology **148**(10): 1467-1477.

Papale, D. and A. Valentini (2003). "A new assessment of European forests carbon exchanges by eddy fluxes and artificial neural network spatialization." Global Change Biology **9**(4): 525-535.

Parton, W. J., M. Hartman, D. Ojima and D. Schimel (1998). "DAYCENT and its land surface submodel: description and testing." Global and Planetary Change **19**(1-4): 35-48.

Parton, W. J., E. A. Holland, S. J. Del Grosso, M. D. Hartman, R. E. Martin, A. R. Mosier, D. S. Ojima and D. S. Schimel (2001). "Generalized model for NOx and N2O emissions from soils." Journal of Geophysical Research-Atmospheres **106**(D15): 17403-17419.

Parton, W. J., J. M. O. Scurlock, D. S. Ojima, T. G. Gilmanov, R. J. Scholes, D. S. Schimel, T. Kirchner, J. C. Menaut, T. Seastedt, E. G. Moya, A. Kamnalrut and J. I. Kinyamario (1993). "Observations and modeling of biomass and soil organic-matter dynamics for the grassland biome worldwide." Global Biogeochemical Cycles **7**(4): 785-809.

Reichstein, M., E. Falge, D. Baldocchi, D. Papale, M. Aubinet, P. Berbigier, C. Bernhofer, N. Buchmann, T. Gilmanov, A. Granier, T. Grunwald, K. Havrankova, H. Ilvesniemi, D. Janous, A. Knohl, T. Laurila, A. Lohila, D. Loustau, G. Matteucci, T. Meyers, F. Miglietta, J. M. Ourcival, J. Pumpanen, S. Rambal, E. Rotenberg, M. Sanz, J. Tenhunen, G. Seufert, F. Vaccari, T. Vesala, D. Yakir and R. Valentini (2005). "On the separation of net ecosystem exchange into assimilation and ecosystem respiration: review and improved algorithm." Global Change Biology **11**(9): 1424-1439.

Ryan, M. G. and R. H. Waring (1992). "Maintenance respiration and stand development in a sub-apline lodgepole pine forest." Ecology **73**(6): 2100-2108.

Sacks, W. J., D. S. Schimel and R. K. Monson (2007). "Coupling between carbon cycling and climate in a high-elevation, subalpine forest: a model-data fusion analysis." Oecologia **151**(1): 54-68.

Sacks, W. J., D. S. Schimel, R. K. Monson and B. H. Braswell (2006). "Model-data synthesis of diurnal and seasonal CO2 fluxes at Niwot Ridge, Colorado." Global Change Biology **12**(2): 240-259.

Schimel, D. S. (1995). "Terrestrial Ecosystems and the carbon-cycle." Global Change Biology **1**(1): 77-91.

Schimel, D. S., T. G. F. Kittel, S. Running, R. K. Monson, A. Turnipseed and D. Anderson (2002). "Carbon sequestration studied in Western U.S. mountains." EOS. Transactions of the American Geophysical Union **83** (40): 445–449.

Sprugel, D. G., M. G. Ryan, J. R. Brooks, K. A. Vogt and T. A. Martin (1995). Respiration from the organ level to the stand. In Resource Physiology of Conifers: Acquisition, Allocation and Utilization., Academic Press, San Diego, CA.

Stephens, B. B., K. R. Gurney, P. P. Tans, C. Sweeney, W. Peters, L. Bruhwiler, P. Ciais, M. Ramonet, P. Bousquet, T. Nakazawa, S. Aoki, T. Machida, G. Inoue, N. Vinnichenko, J. Lloyd, A. Jordan, M. Heimann, O. Shibistova, R. L. Langenfelds, L. P. Steele, R. J. Francey and A. S. Denning (2007). "Weak northern and strong tropical land carbon uptake from vertical profiles of atmospheric CO(2)." Science **316**(5832): 1732-1735.

Tans, P. P., I. Y. Fung and T. Takahashi (1990). "Observational constraints on the global atmospheric CO2 budget." Science **247**(4949): 1431-1438.

Turnipseed, A. A., D. E. Anderson, P. D. Blanken, W. M. Baugh and R. K. Monson (2003). "Airflows and turbulent flux measurements in mountainous terrain Part 1. Canopy and local effects." Agricultural and Forest Meteorology **119**(1-2): 1-21.

Turnipseed, A. A., D. E. Anderson, S. Burns, P. D. Blanken and R. K. Monson (2004). "Airflows and turbulent flux measurements in mountainous terrain Part 2: Mesoscale effects." Agricultural and Forest Meteorology **125**(3-4): 187-205.

Turnipseed, A. A., P. D. Blanken, D. E. Anderson and R. K. Monson (2002). "Energy budget above a high-elevation subalpine forest in complex topography." Agricultural and Forest Meteorology **110**(3): 177-201.

Wang, Y. P. and D. J. Barrett (2003). "Estimating regional terrestrial carbon fluxes for the Australian continent using a multiple-constraint approach I. Using remotely sensed data and ecological observations of net primary production." Tellus Series B-Chemical and Physical Meteorology **55**(2): 270-289.

Weiskittel, A. R., D. A. Maguire, S. M. Garber and A. Kanaskie (2006). "Influence of Swiss needle cast on foliage age-class structure and vertical foliage distribution in Douglas-fir plantations in north coastal Oregon." Canadian Journal of Forest Research-Revue Canadienne De Recherche Forestiere **36**(6): 1497-1508.

Zobitz, J. M., D. J. P. Moore, W. J. Sacks, R. K. Monson, D. R. Bowling and D. S. Schimel (2008). "Integration of process-based soil respiration models with whole-ecosystem CO2 measurements." Ecosystems **11**(2): 250-269.